# Extracting spatiotemporal characteristics and succession pattern of native and invasive plant species using plant phenophase and multi-source remote sensing images in the Yellow River delta, China

Zhaoning Gong[1], Cheng Zhang[1], Lei Zhang[1], Junhong Bai[2], and Demin Zhou[1]

[1]Capital Normal University
[2]Beijing Normal University

April 28, 2020



**Abstract**

The native and invasive species in the Yellow River Delta were examined for their spatiotemporal characteristics and succession pattern. First, the appropriate Sentinel-2 and Landsat-8 images from 2018 were selected according to phenological characteristics. A random forest algorithm was used to verify the image spectral band significance and separability using selected images to determine the native and invasive species. Then, the spatiotemporal variation of habitat structure of native and invasive species is discussed in depth from the perspective of landscape ecology. Finally, the expansion direction and expansion mode of S. alterniflora were further analyzed, and main results were obtained as follows. (1) At the medium-high resolution multispectral image level, the accuracy of different vegetation community extractions can be improved by taking into consideration both the vegetation phenology and the spectral features of remote sensing images. (2) Sentinel-2 images with red edge bands have obvious advantages in vegetation community extraction as compared to Landsat-8 images (Sentinel-2, OA=82.86%, Kappa coefficient=0.79; Landsat-8, OA=78.77%, Kappa coefficient=0.74). (3) The expansion pattern of the S. alterniflora community became spatially continuous, more regularized and aggregated overtime. (4) The expansion in the north shore mainly faces to the sea, and the south bank mainly faces to the land, and this phenomena is closely related to the sedimentation of the Yellow River Delta. Marginal and external expansion both occurred, but marginal expansion predominated. The results from this study have important theoretical and scientific value for the environmental protection and sustainable development of the entire Yellow River Delta.

**Extracting spatiotemporal characteristics and succession pattern of native and invasive plant species using plant phenophase and multi-source remote sensing images in the Yellow River delta, China**

**Zhaoning Gong [1, 2, 3, 4], Cheng Zhang[1, 2, 3, 4], Lei Zhang [1, 2, 3, 4]** 11* Corresponding authors.*E-mail addresses:* zhangleigis@outlook.com**, Junhong Bai[5], Demin Zhou[1, 2, 3, 4]**

[1] College of Resources, Environment and Tourism, Capital Normal University, Beijing 100048, China

[2] Key laboratory of 3D Information Acquisition and Application of Ministry, Beijing 100048, China

[3] Beijing Key Laboratory of Resources Environment and GIS, Beijing, 100048, China

[4] Beijing Laboratory of Water Resources Security, Beijing, 10048, China

[5] College of Environment, Beijing Normal University, Beijing, 100875, China

Abstract: The native and invasive species in the Yellow River Delta were examined for their spatiotemporal characteristics and succession pattern. First, the appropriate Sentinel-2 and Landsat-8 images from 2018

were selected according to phenological characteristics. A random forest algorithm was used to verify the image spectral band significance and separability using selected images to determine the native and invasive species. Then, the spatiotemporal variation of habitat structure of native and invasive species is discussed in depth from the perspective of landscape ecology. Finally, the expansion direction and expansion mode of *S. alterniflora* were further analyzed, and main results were obtained as follows. (1) At the medium-high resolution multi-spectral image level, the accuracy of different vegetation community extractions can be improved by taking into consideration both the vegetation phenology and the spectral features of remote sensing images. (2) Sentinel-2 images with red edge bands have obvious advantages in vegetation community extraction as compared to Landsat-8 images (Sentinel-2, OA=82.86%, Kappa coefficient=0.79; Landsat-8, OA=78.77%, Kappa coefficient=0.74). (3) The expansion pattern of the*S. alterniflora* community became spatially continuous, more regularized and aggregated overtime. (4) The expansion in the north shore mainly faces to the sea, and the south bank mainly faces to the land, and this phenomena is closely related to the sedimentation of the Yellow River Delta. Marginal and external expansion both occurred, but marginal expansion predominated. The results from this study have important theoretical and scientific value for the environmental protection and sustainable development of the entire Yellow River Delta.

Key words: multi-source remote sensing images; plant phenophase; temporal and spectral characteristics; invasive species; expansion analysis; the Yellow River Delta wetland



# 1. Introduction

Invasive species are considered to be the second largest factor in global biodiversity reduction after habitat destruction, have significant advantages in terms of growth, reproduction, and competition, and can pose a great threat to local ecosystems (Liu et al.2015). The estuary wetland, located at the sea-land junction of the river and the sea, is an ecological marginal zone formed by two distinct ecosystems. This ecosystem is so sensitive and fragile that it is a frequent area for biological invasion (Wang 2005). The Yellow River Delta Wetland, as a typical estuary wetland in northern China, appeared in the "List of Ramsar wetlands of international importance" by the Ramsar Convention on Wetlands in 2013. It is not only one of the most representative estuarine wetlands in the world, but it is also the most complete and the vastest, youngest wetland ecosystem in the warm temperate zone of China (Gong et al.2016; Wen et al.2011).

Smooth cordgrass (*Spartina alterniflora* ) is an invasive plant that was artificially introduced. It exerts a certain degree of wind protection, berm protection, beach preservation, and siltation in the estuary wetland in the early stage. *S. alterniflora* has been introduced into many countries throughout history, including the west coast of North America, Europe, New Zealand, and China, and it has spread rapidly at all these introduction sites(Chen, et al., 2004; Deng et al., 2006). *S. alterniflora* was introduced into China as an ecological project in 1979. However, *S. alterniflora* has strong salt and reproductive capacity. At the same time, it lacks competing species and natural enemies along the coast of China, which has resulted in a great expansion of *S. alterniflora* in China's coastal areas.. It has gradually encroached on the living space of the native marsh plant species, which consists of seepweed (*Suaeda salsa* ) and the common reed (*Phragmites australis* ), and it has caused serious damage to the original ecosystem of the Yellow River Delta (Zhou et al.2017). Therefore, it is urgent to use advanced technology to timely monitor the distribution patterns and trends of the native and invasive plant species in the Yellow River Delta, which will provide a scientific basis for the protection and rational use of wetland resources in the future.

Compared with field research, remote sensing (RS) technology has the advantages of wide observation range, flexible monitoring period, and large amount of information. These technologies were widely used in many studies in China. For example, saltmarsh vegetation types were mapped and analyzed based on remote sensing images with an ideal precision (Huang et al. 2007; Sun et al. 2016;Ai et al. 2016). Combined with vegetation phenological characteristics, Wu et al. (2012) used Landsat and Moderate Resolution Imaging Spectroradiometer (MODIS) satellite data to obtain vegetation indexes to track the expansion of *S. alterniflora* in the coastal area of the southern Yellow Sea. Wan et al. (2010) collected HJ-1 charge-coupled device

(CCD) images and high-resolution unmanned aerial vehicle (UAV) images in the Guangxi Beihai area, and extracted the distribution pattern of *S. alterniflora* . The results indicated that the UAV image can provide detailed information on the distribution range and expansion process of*S. alterniflora* . Under the support of 3S (GIS, GPS, and RS) technology, Wang et al. (2018) analyzed the spatial distribution characteristics of *S. alterniflora* in Jiangsu Yancheng National Nature Reserve from 2006 to 2015 through the landscape index and centroid change, and then they used Gaofen-2 (GF-2) satellite images to identify the expansion pattern of *S. alterniflora* and predict the expansion trend. The above research on *S. alterniflora* has been conducted mainly in southern China. Since 2010, *S. alterniflora*has invaded beaches and expanded its range, but there are few studies on the growth scale, habitat structural changes, and expansion pattern of*S. alterniflora* in the Yellow River Delta.

With the improvement in Earth observation systems in the 21$^{st}$ century in various countries and regions, an increasing number of remote sensing images have surpassed the limitation of the number of bands, spatial resolution, and revisiting cycles (Zheng et al. 2017). The long-sequence terrestrial satellite Landsat has become one of the common sources of multi-source imagery, and the twin Sentinel-2 satellites launched by the European Space Agency (ESA) are also becoming widely used in research. Tesfamichael et al. (2017) compared multi-band remote sensing images (Landsat-8, Sentinel-2A, Spot-6, Pleiades-1B, and WorldView-3) to distinguish three intrusions of shrub plants from native plants that are symbiotic with shrub plants.

Compared to the Landsat series of data, the two Sentinel-2 satellites are equipped with a Multispectral Instrument (MSI), which provides remote sensing images with multi-scale, medium-high spatial resolution (10 m, 20 m, and 60 m) from visible and near-infrared to short-wave infrared (13 bands). Moreover, the Sentinel-2 satellites specifically monitor three bands in the red edge region (670-760 nm) of the vegetation spectrum, which is very effective for monitoring vegetation growth information and its health status (Shoko et al. 2017; Delegido et al. 2011; Korhonen et al. 2017). At the same time, the revisiting cycle of the two Sentinel-2 satellites was shortened to 5 days, which greatly enhances the capability for Earth observation (Zheng et al. 2017). Therefore, how to exploit the advantages of the two Sentinel-2 satellites in monitoring the surface of the Earth is bound to become the focus of future research in global scientific research.

In view of this, it is imperative that we build a capacity to monitor timely the spatial and temporal characteristics of the invasive plant species and their dynamic changes in order to restore ecological conditions and protect the environment in the Yellow River Delta. The main objectives of this study are to characterize the spatial distribution and spatiotemporal variation of native/invasive species via remote sensing and to understand the expansion mechanism of *S. alterniflora* in the Yellow River Delta, which are the key point in the restoration and reconstruction of the estuary wetland ecosystem.

The following analyses were conducted to meet the objectives of this study:

(1) Conducting spectral feature selection using Sentinel-2 images and Landsat-8 images acquired at different phenological stages of the native and invasive species in 2018 in the Yellow River Delta. The selection process was accomplished by using a random forest algorithm.

(2) Based on selected spectral bands of Sentinel-2 and Landsat-8 images of 2018, the native and invasive species of the Yellow River Delta were extracted and mapped using a random forest classifier and results were validated using reference data.

(3) Based on results from step (1) and (2), the temporal and spatial variations of native and invasive species were quantified and analyzed, and the main expansion directions and expansion patterns of the *S. alterniflora* community were examined from the perspective of landscape ecology.

# 2. Materials and Methods

## 2.1 Study area

The Yellow River Delta (118°32.981'E—119deg20.450'E and 37deg34.768'N—38deg12.310'N), which is located at the estuary of the Yellow River in Dongying City, Shandong Province, China (Fig. 1a-c), is one of China's four largest river deltas. As a national nature reserve, it was officially listed on the international list of important wetlands in 2013. The delta, bounded by the Bohai Sea in the north and the Laizhou Bay in the east, has a typical temperate monsoon climate with four distinct seasons, and rain and heat over the same period. The average annual temperature is 12.1degC, the precipitation is 530–630 mm, and the evaporation is 1900–2400 mm in the study area (Liu et al. 2017; Shandong Yellow River Delta National Nature Reserve Administration 2016). Despite the flat topography, the ecological pattern varies with time and space, and the types of wetlands are diverse in this region.

## 2.2 Data acquisition

### 2.2.1 Remote sensing data and image preprocessing

Due to the complex habitat information and seasonal succession of estuary wetlands, three Sentinel-2 images and three Landsat-8 images taken under clear weather conditions were selected to test their ability in discriminating between native species and invasive species. The Sentinel-2 satellite images used in this study were recorded on May 27, 2018, September 09, 2018, and October 19, 2018. In order to reduce the differences caused by different times, Landsat-8 satellite images with times similar time to those of the Sentinel-2 images were selected, and images were used that were produced on May 28, 2018 (Sentinel-2A), September 17, 2018 (Sentinel-2B), and October 19, 2018 (Sentinel-2B). The data is introduced in Surpppporting Imformation part2(S2).

### 2.2.2 Sample data and validation data

The quality of the sample data is directly related to the accuracy of the native and invasive species extraction (Liu et al. 2017). A typical and representative pure pixel was selected as the sample. The data in this study mainly come from on-site field surveys and visual interpretation based on high-resolution images such as those from Google Earth. From 2017 to 2018, the experimental group conducted a detailed survey of the Yellow River Delta Nature Reserve, using high-precision GPS to locate, record, and photograph different vegetation communities. At the same time, a part of the native and invasive species was visually interpreted indoors through Google Earth software and the MAP WORLD website. The above two parts of the data constitute the sample data and verification data for the establishment of the classifier and the accuracy verification. The distribution and specific sources of sample data and verification data are shown in Table 1.

*Methods are introduced in the S3.

# 3. Results and Analyses

## 3.1 Selection of feature bands

The band importance index was extracted by the random forest algorithm (Fig. 2). Sentinel-2 images have approximately four to five bands of higher importance in all three months, particularly, the red-edge band (B06, B07) and near-infrared band (B08A) are more important. Compared to Sentinel-2 images, Landsat-8 images have approximately two to three bands of higher importance in all months, especially the red-band (B04) and near-infrared band (B05). The importance of the near-infrared band in May is particularly prominent.

The importance index of the band can only determine the contribution of different bands. In order to reduce the noise generated by the band with a lower contribution rate, we determined for each image if there are any important bands for species extraction. The bands of the top n importance at different months were selected as the basis for separating different species. If the importance of a band at the given time is ranked as the top one, but its separability is poor, other bands from the same image with a lower importance index can be considered as a noise band that should be discarded. The bands that are selected with higher separability are those that will be used for final extraction.

Figure 3 shows the spectral separability of the n significant bands of Sentinel-2 images for different months. For example, during the corresponding phenological stage, the red edge band (B06, B07) and the near-infrared band (B08A) of the vegetation can be used to effectively distinguish between *S. salsa* , *P. australis* , and *S. alterniflora.* Among them, 09_B06, 09_b07, 09_B08A, and 10_B08A can basically achieve separation between the three species. We selected multi-temporal bands with good separability from the Sentinel-2 source data (05_B06, 05_B07, 05_B08A, 05_B12, 09_B08A, 09_B07, 09_06, 09_02, 09_B04, 10_B06, 10_B08A, 10_B12, 10_B11, 10_B04, 10_02, and 10_07) to extract the native and invasive species of the study area.

The Landsat-8 image spectral separability band is mainly concentrated in the red band (B04) and the near-infrared band (B05) (Fig. 4). From the importance and separability analysis of the bands, it was found that the Landsat-8 image in September had the best separability and the most bands (09_B04, 09_B05, 09_B01, 09_B02, and 10_B04) for *S. salsa* ; however, there were only two separable bands for *P. australis* (05_B05, 05_B07) and one for *S. alterniflora*(10_B05).

The above analysis shows that the multi-temporal Landsat-8 and Sentinel-2 images can distinguish *S. salsa* , *P. australis* , and *S. alterniflora* . The spectral separability bands were mainly concentrated in the red band (630 nm-680 nm, Landsat-8), near-infrared band (845 nm-885 nm, 848 nm-880 nm, Landsat-8, Sentinel-2), and vegetation red edge band (739 nm-749 nm, 768 nm-796 nm, Sentinel-2). Besides, some studies have shown that the multi-temporal vegetation index (such as NDVI) of the Landsat-5 image can also distinguish between the three types of vegetation (Wang et al. 2013).

## 3.2 Classification and accuracy analysis

Figure 5 shows the native and invasive species extracted from Landsat-8 images and Sentinel-2 images. It can be seen from the figure that the distribution patterns of *S. salsa* , *P. australis* , and*S. alterniflora* shown in the two images are almost the same.*P. australis* is predominant on the beaches on both sides of the Yellow River and the artificially restored recovery areas. *S. salsa* is mainly distributed in the beaches and areas of high salinity in the Yellow River Delta. It is a pioneer plant in muddy tidal flats and heavy saline-alkaline areas. *S. alterniflora* mainly grows in the lower part of the intertidal zone to the lower part of the middle tide zone.

The overall accuracy of data extraction based on multi-temporal Sentinel-2 is 82.86%, with a Kappa coefficient of 0.79; the overall accuracy of data extraction based on multi-temporal Landsat-8 is 78.77%, with a Kappa coefficient of 0.74 (Tab. 2). Regardless of the image, the producer accuracy and user accuracy of *S. salsa* and*S. alterniflora* are generally higher than those of *P. australis* , which is caused by many factors, such as plant height, plant density, and the type of underlying surface. However, *P. australis* and *S. alterniflora* exhibit a mixed phenomenon, and the extraction accuracy is low in the areas with more human activities. When the Landsat-8 image is used for classification, the *P. australis* growth is misclassified into that of *S. alterniflora*in the marginal areas where the reed grows, but this problem does not occur in Sentinel-2 images.

## 3.3 Analysis of landscape dynamics related to native and invasive species

The results of the extraction of native and invasive species in the Yellow River Delta wetlands for 2010, 2013, 2016, and 2018 are shown in Figure 7. The growth area for *P. australis* is 66.96 $km^2$, 63.84 $km^2$, 76.26 $km^2$, and 72.73 $km^2$ for 2010, 2013, 2016, and 2018, respectively, and the area change shows a steady upward

trend. The area where *S. salsa* is found covers 47.6 $km^2$, 27.48 $km^2$, 39.61 $km^2$, and 35.04 $km^2$ in the same four time periods, respectively, which shows a downward trend. *S. alterniflora* greatly expanded its range from 2010 to 2016, rapidly increasing from 1.14 $km^2$ to 30.77 $km^2$. The expansion trend slowed from 2016 to 2018, but the area still reached 40.53 $km^2$ in 2018.

Due to the influence of tidal currents, large areas of beaches are flooded during the high tide, which results in the death of some earlier growth of*S. salsa* . After the ebb tide, the seeds of*S. salsa* sprout, and new seedlings are re-grown. The *S. salsa*community in the adjacent part of the sea reciprocates with the tide period, and poor growth is exhibited mainly in the decreased density and short size of the plants. Therefore, the patch density and splitting index of *S. salsa* were significantly higher than that of *P. australis* and *S. alterniflora* , and the aggregation index is the lowest (Fig. 2), which indicates that the spatial distribution of*S. salsa* is irregular and discrete. With the passage of time, the patch density of *S. salsa* is decreased, but the splitting index is always at a high level, which indicates that the area of *S. salsa* in the study location is gradually decreasing, and the poor growth conditions lead to severe fragmentation of the spatial distribution.

Over the past 10 years, the landscape indices of the*P. australis* community have been relatively stable, without a sharp change. The patch density was low, the largest patch index was the highest among the three vegetation communities, and the aggregation index was also stable at approximately 90. This occurred because a large number of wetland ecological restoration projects have been carried out in the Yellow River Delta region, and *P. australis* gradually formed a contiguous distribution pattern based on its rapidly expanding reproductive capacity, becoming an emergent aquatic plant community of a single dominant species.

Growth of *S. alterniflora* was recorded in the estuary of the Yellow River at the beginning of the $21^{st}$ century. Due to the impact of the tidal runoff and the Yellow River diversion, initially, there was no large-scale expansion of*S. alterniflora* . At present, under the influence of water and sediment adjustment in the upper reaches of the Yellow River, the area of the *S. alterniflora*community has been rapidly expanding. Since 2010, the patch density, largest patch index, and aggregation index of *S. alterniflora*have shown an upward trend, with the splitting index showing a significant downward trend, which highlights that the area of occupation for *S. alterniflora* is gradually increasing. The spatial distribution of the community gradually shows a pattern of continuous, regularized, and integrated growth. A number of previous researchers have reported that *S. alterniflora* currently appears only on both sides of the Yellow River estuary. An area of *S. alterniflora*growth was found in the southern tidal flat for the first time in this study. There was only a sporadic distribution in the 2017, but a pattern of small-scale contiguous distribution was observed in 2018 (Fig. 7).

## 3.4 Analysis of expansion of S. alterniflora community

### 3.4.1 Expansion direction analysis

To study expansion direction of *S. alterniflora* from 2010 to 2018, the relevant parameters of the standard deviation ellipse of*S. alterniflora* were obtained. There were great changes in the spatial distribution pattern of *S. alterniflora* on the north bank of the Yellow River estuary. The movement path underwent a change consisting of "Northwest (2010-2013)—Northeast (2013-2016)—Northwest (2016-2018)," which generally shows a trend of moving to the northwest. The standard deviation of the elliptical distribution range of *S. alterniflora* showed an expanding trend from 2010 to 2018. The long semi-axis and the short semi-axis increased from 0.52 km and 0.12 km in 2010 to 83.86 km and 19.17 km in 2018, respectively. Combining the change of the long and short half-axis and the distribution pattern of the standard deviation ellipse shows that the distribution of *S. alterniflora* on the north shore is dominated by movement in the east-west direction. During the study period, the standard deviation of the elliptical deflection angle of the north shore ranged from 89.35deg to 108.81deg.

The center of gravity of *S. alterniflora* on the south bank of the Yellow River is mainly north-south, with small movements from east to west. It moved mainly to the south in 2010–2013 and moved northward in 2013–2018. The long semi-axis and the short half-axis increased from 0.66 km and 0.11 km in 2010 to 39.01

km and 15.66 km in 2018, respectively. The distribution of the *S. alterniflora* community on the south bank is mainly in the north-south direction. Compared with the north shore, the deflection angle of the south bank has been decreasing, from 75.81deg in 2010 to 2.78deg in 2018, which indicates that the *S. alterniflora* community on the south bank is mainly oriented towards land expansion.

### 3.4.2 Analysis of Expansion mode

Zhang et al.(2018) studied the diffusion mechanism of *S. alterniflora* from the perspective of genetic evolution. The study showed that all the *S. alterniflora* communities in this study area are from the No. 5 pile area, rather than gradually expanding from the north bank of the Yellow River estuary to the south bank, which indicates that the genetic distance of*S. alterniflora* has no relationship with the geographical distance. The seeds of *S. alterniflora* can be transported over long distances by seawater for plant propagation. After determining the source of the expansion of*S. alterniflora* , subsequent studies herein mainly analyzed the different expansion patterns after *S. alterniflora* colonization.

The multi-year expansion pattern obtained by using the LEI index shows that from the expansion area, the main expansion mode of the *S. alterniflora* community in the past 10 years is edge expansion. This mode of expansion is characterized by the outward expansion of the marginal region of the patches extracted from the previous phase, which is adjacent to the native patches. The total area of edge expansion is 33.97 $km^2$, and the expansion area is larger than the original block area (0[?]LEI<1). The external expansion area is small, with a total area of 5.42 $km^2$, and the new*S. alterniflora* patches are not adjacent to other *S. alterniflora* patches, which demonstrates a discrete distribution state. However, from the number of patches, the number of edge expansion plaques in the *S. alterniflora* community is slightly less, only 73, and the total number of external expansion patches is 339, which also indicates that the growth scale of *S. alterniflora* community is continuous, regularized, and integrated.

# 4. Discussion

4.1 Image Analyses and Species Classification

Based on the multi-temporal Sentinel-2 imagery and Landsat imagery, the extraction of the dominant species in the Yellow River Delta can be achieved by the more important bands optimized by the random forest algorithm. There were significantly more bands with more importance from Sentinel-2 images than those from Landsat images, which is mainly due to the fact that the three unique red-edge bands of Sentinel-2 images provide more data support for the spectral separability of different species. This resulted in an overall accuracy of the Sentinel-2 image extraction results that was slightly higher than that for the Landsat images. Both types of data have advantages and disadvantages when extracting native and invasive species. Sentinel-2 data can improve the classification accuracy by the advantages of band and spatial resolution. The Landsat data can make up for the shortcomings of Sentinel-2 data in long-term sequences. The combination of the two images enabled us to analyze the temporal and spatial variation of native and invasive species in the study area.

For extracting *S. salsa* in current study area, remote sensing image of September was selected because of the following reasons: (1) Studies have shown that the key substance for the discoloration of*S. salsa* is salt. When *S. salsa* grows in a low salt environment (0.3–1%), the vacuole tissue of its leaf cells is mainly chlorophyll. However, in strong salinity (1–1.6%), betaine becomes the main vacuole structure, which results in leaves that appear red. (2) In September, it is in the middle growth stage of*S. salsa* , with high biomass and a wide distribution area. At the beginning of September, the Chinese rain belt begins to rapidly withdraw south, with cold air remaining in the north. The rainy season in North China ends, the amount of water coming from the Yellow River decreases, the groundwater depth subsequently decreases, and the soil salinity increases. The various factors mentioned above lead to the change of color of *S. salsa*from reddish to fuchsia

in September, which can better highlight the difference in remote sensing images between *S. salsa* and other vegetation.

As can be seen from Figure 7 that the distribution pattern of native and invasive species has obvious gradients. The main driving forces for this distribution and succession are water (groundwater depth), salt (soil salinity), and human activities. The study area is located where river freshwater and seawater interact. From the river bank highland to the intertidal zone, the freshwater wetland is gradually transformed into saltwater wetland, and the water and salt distributions have obvious gradient differentiation. Since the *S. salsa* , *P. australis* , and *S. alterniflora* communities can only survive under certain water and salt conditions, the existence of water and salt gradients leads to the distribution and succession of the three communities with obvious zonal distribution. At the same time, the ecological restoration projects of the constructed wetland in the protected area will funnel the freshwater of the Yellow River into the ecological restoration area, which will increase the groundwater depth in this area. The salt washing and salt discharging actions by fresh water will reduce the degree of soil salinization. These conditions were suitable for the reed community, and promoted its growth so that it became the dominant species in the ecological restoration area.

Regardless of the landscape index or expansion analysis, the expansion of the *S. alterniflora* community has become an indisputable fact. According to the current research results, the expansion of the north shore is mainly manifested as expansion to the sea. This is because rivers flowing eastward in the northern hemisphere are affected by the Earth's rotation, which will cause washing of the south bank of a river. However, sediment will be deposited due to the slower water flow in the north shore. It is the sedimentation on the north shore that provides habitat conditions for the rooting and wild growth of *S. alterniflora* . The data provided by the Lijin hydrological station (the nearest hydrological station in the Yellow River Delta) show that the artificial water and sediment adjustment occurring in the upper reaches of the Yellow River in 2010 and 2013 resulted in a large amount of sediment deposited on the north bank of the Yellow River estuary, which led to a significant increase in the area of the *S. alterniflora*community on the north shore in 2013 and 2016.

The data show that water and sediment adjustment has increased in 2018, and sedimentation in the northern part of the Yellow River estuary can be visualized from remote sensing images. It is foreseeable that in the next two years, the expansion of *S. alterniflora* on the north bank of the Yellow River estuary will still be considered to be on the sea side. There is less sedimentation in the south bank, and therefore, the expansion of *S. alterniflora* occurred mainly towards the land. The expansion pattern indicates that the *S. alterniflora*community is dominated by marginal expansion. This expansion relies mainly on underground roots for tillering, while the highly developed and aerated tissue of *S. alterniflora* provides sufficient oxygen to its roots to facilitate the growth of adjacent *S. alterniflora*plants. The external expansion area is small, but the number of patches is high. This type of expansion is very important for the development of plant growth in a new environment.

4.2 Biological and Ecological Impacts

The reproductive ability, high tolerance and adaptability to tidal flat environmental stress of *S. alterniflora* determine its competitive advantage in the intertidal zone. Due to its high tolerance to flooding and salinity, *S. alterniflora* has an absolute competitive advantage on the coastal side. When external factors such as tide carry the seeds of *S. alterniflora* to a new habitat, *S. alterniflora* colonizes in a new habitat, depending on sexual reproduction, and begins the external expansion. Because of its low productivity in the early stage of colonization, its patch area is relatively small and scattered. After the successful establishment of*S. alterniflora* , the seedlings are difficult to survive due to the low light intensity under the canopy of the community. Therefore,*S. alterniflora* starts a rapid marginal expansion relying on asexual reproduction, forming a large area of single-spices community with high density and productivity, which prevents other vegetation from growing in its distribution area (Wang Q, 2006).

The external expansion patches in the southernmost tidal flat may be caused by the spread of seawater or ships and birds. It is expected that*S. alterniflora* will gradually occupy the southern light beach in the next

few years. The tide is one of the carriers of *S. alterniflora* seeds. The development of tidal creek can promote the external expansion of *S. alterniflora* . *S. alterniflora*seeds drift with the tide and germinate and settle on the edge of the tidal creek, and invades along the tide to the land side. In addition, due to the strong shore-fixing ability of *S. alterniflora* , the erosion of the tide creek by the tide has changed from horizontal to vertical, forming a narrow and deep tide creek (Shen Y M, 2003;Zhaoning Gong, 2019). *S. alterniflora* has a certain wave-slowing effect, which can promote bank consolidation, but it also affects the development of tidal creek and is not conducive to hydrological connectivity. In addition, the invasion of *S. alterniflora* has reduced the distribution of native species, endangered biodiversity, occupied the light beach, and caused the loss of bird habitats and food sources, such as rare birds — red-crowned cranes and black-billed gulls that depend on the habitat of Suaeda salsa(Gallardo B,2016; Callaway J C,1992; Guy-Haim T,2018). Prevention and management measures should be taken in time to suppress the invasion of *S. alterniflora* .

# 5. Conclusions

The results from this study demonstrate that it is feasible to extract native and invasive species in the Yellow River Delta region based on phenological characteristics of vegetation and spectral features of satellite remote sensing images. May and October are important periods for extracting the *P. australis* community and the *S. alterniflora* community, respectively, in the Yellow River Delta or in the coastal wetlands in North China. The landscape characteristics and spectral characteristics of the two communities are not much different and are difficult to distinguish.

The accuracy of different vegetation community in this area can be improved by taking into consideration both the vegetation phenology and the spectral features of remote sensing images. The Sentinel-2 images with red edge bands have obvious advantages in vegetation community extraction as compared to Landsat-8 images. The *P. australis*community in the study area is the dominant species, and its multi-year landscape index is stable. The spatial distribution of *S. salsa*is discrete, the degree of aggregation is low, and the area is decreasing. The landscape index of the *S. alterniflora* community showed a trend of increasing year by year, but the degree of fragmentation decreased, indicating that the expansion pattern of the*S. alterniflora* community became spatially continuous, more regularized and aggregated overtime.

The findings from this study advanced understanding of the spatial distribution and spatiotemporal variation characteristics of native and invasive plant species, and the expansion mechanism of *S. alterniflora* and other species in the study area, and provide a basis for making scientifically sound decision for management and the control*S. alterniflora* invasion. It will contribute to the ecological restoration and the protection of species diversity of the entire Yellow River Delta in China. In addition, the research findings have important theoretical and scientific value for the ecological environment protection and sustainable development of the worldwide estuary wetland ecosystem.

# Acknowledgements

This work was supported by the Project of National Keypoint Research and Invention Program of "13th Five Year" Period (2017YFC0505900) . The authors greatly thank Limin Yang (Guest Professor, Capital Normal University, Beijing, China) ) for revising and editing the contents of the paper in English.

# References

Ai J, Gao W, Gao ZQ, et al. (2016). Errata: Integrating pan-sharpening and classifier ensemble techniques to map an invasive plant (Spartina alterniflora) in an estuarine wetland using Landsat 8 imagery. Journal of Applied Remote Sensing. DOI: 10.1117/1.JRS.10.029901

Callaway J C, Josselyn M N. (1992). The introduction and spread of smooth cordgrass (Spartina alterniflora) in South San Francisco Bay. Estuaries 15(2): 218–226.

Chen, Z.; Li, B., and Chen, J. (2004). Ecological consequences and management of Spartina spp. invasions in coastal ecosystems. Chinese Biodiversity, 12(2), 280-289.

Delegido, J., Verrelst, J., Alonso, L. and Moreno, J. (2011). Evaluation of sentinel-2 red-edge bands for empirical estimation of green lai and chlorophyll content. Sensors, 11(7), 7063-81.

Deng, Z.F.; An, S.Q.; Zhi, Y.B.; Zhou, C.F.; Chen, L.; Zhao, C.J., and Li, H.L. (2006). Preliminary studies on invasive model and outbreak mechanism of exotic species, Spartina alterniflora Loisel. Acta Ecologica Sinica, 26(8), 2678-2686.

Gallardo B, Clavero M, Sanchez MI, et al. (2016). Global ecological impacts of invasive species in aquatic ecosystems. Global Change Biology, 22(1):151-163.

Gong N, Niu Z G, Qi W and Zhang H Y. (2016). Driving forces of wetland change in China. Journal of Remote Sensing, 20(2): 172–183. DOI: 10.11834/jrs.20164210 (in Chinese)

Guy-Haim T, Lyons DA, Kotta J, et al. (2018). Diverse effects of invasive ecosystem engineers on marine biodiversity and ecosystem functions: A global review and meta-analysis. Global Change Biology, 24(3):906-924.

Huang H, Zhang L. (2007). A study of the species dynamics of Spartina alterniflora at Jiuduansha shoals, Shanghai, China. Ecological Engineering, 29(2):164-172.

Korhonen L, Hadi, Packalen P and Rautiainen M. (2017) Comparison of Sentinel-2 and Landsat 8 in the estimation of boreal forest canopy cover and leaf area index. Remote Sensing of Environment, 195:259-274.

Liu H Y, Lin Z S, Qi X Z, Liu J X, Xu X J. (2015) The dispersal mechanism of invasive plants based on a spatially explicit individual-based model and Remote sensing technology: a case study of Spartina alterniflora.Acta Ecologica Sinica, 35(23): 7794-7802. (in Chinese)

Liu L, Han M, Liu Y B, Pan B. (2017) Spatial distribution of wetland vegetation biomass and its influencing factors in the Yellow River Delta Nature Reserve. Acta Ecologica Sinica, 37(13):4346-4355. (in Chinese)

Liu S ,Jiang Q G, Ma Y, Xiao Y, Li Y H, Cui c. (2017) Object-oriented Wetland Classification Based on Hybrid Feature Selection Method Combining with Relief F, Multi-objective Genetic Algorithm and Random Forest. Transactions of the Chinese Society for Agricultural Machinery 48(01):119-127. (in Chinese)

Shandong Yellow River Delta National Nature Reserve Administration (2016) Detailed Planning of National Nature Reserve in the East Yellow River Delta. (in Chinese)

Shen Y M, Zhang R S, Wang Y H, et al. (2003). The tidal creek character in salt marsh of Spartina alterniflora Loisel on strong tide coast. Geographical Research, (04):520-527.

Shoko, C., and Mutanga, O. (2017). Examining the strength of the newly-launched sentinel 2 msi sensor in detecting and discriminating subtle differences between c3 and c4 grass species. Isprs Journal of Photogrammetry & Remote Sensing, 129, 32-40.

Sun C, Liu Y, Zhao S, et al. (2016). Classification mapping and species identification of salt marshes based on a short-time interval NDVI time-series from HJ-1 optical imagery. International journal of applied earth observation and geoinformation, 45: 27-41.

Tesfamichael S G, Newete S W, Adam E, et al. (2017). Field spectroradiometer and simulated multispectral bands for discriminating invasive species from morphologically similar cohabitant plants. GIScience & Remote Sensing, 55(03): 417-436.

Wang C, Liu H Y, Hou M X, Tan Q M. (2013). Classification Method of Muddy Tidal Flat Wetlands Based on Remote Sensing. Journal of Geo-Information Science, 15(04):590-596. (in Chinese)

Wang J, Liu H Y, Li Y F, Liu L, Xie F F. (2018). Recognition of spatial expansion patterns of invasive Spartina alterniflora and simulation of the resulting landscape changes. Acta Ecologica Sinica, 38(15): 5413-5422. (in Chinese)

Wang S G. (2005). Study on Landscape Spatio-temporal Evolution and its-Regulation Countermeasures of the Typical Wetlands in the Pearl River Estuary Region, South China [D], Sun Yat-sen University. (in Chinese)

Wang Q, An S Q, MA Z J, et al. (2006). Invasive Spartina alterniflora: biology, ecology and management. Acta Phytotaxonomica sinica, 44(05):559-588.

Wan Huawei, Wang Changzuo, Li Ya, et al. (2010). Monitoring an invasive plant using hyperspectral remote sensing data [J].Transactions of the CSAE, 26(Supp.2): 59-63. (in Chinese)

Wen Q K, Zhang Z X, Xu J Y, Zuo L J, Wang X, Liu B, Zhao X L and Yi L. (2011). Spatial and temporal change of wetlands in Bohai rim during 2000-2008: An analysis based on satellite images. Journal of Remote Sensing, 15(1):183-200. (in Chinese)

Wu P F, Zhou D M, Gong H L.(2012). A new landscape expansion index: definition and quantification. Acta Ecologica Sinica, 32(13): 4270-4277. (in Chinese)

Yaqian W , Xiangming X , Bangqian C , et al. Tracking the phenology and expansion of Spartina alterniflora coastal wetland by time series MODIS and Landsat images[J]. Multimedia Tools and Applications, 2018.

Zhang L W, Zhao Y J, Wang A D, Feng G M, Song J B, Xie B H, Han G X, LV J Z, Zhu S Y. (2018). Genetic Variation and Spread of Spartina alternifora in the Yellow River Delta. Wetland Science, 16(01):1-8. (in Chinese)

Zhaoning Gong, Qiwei Wang, Hongliang Guan, et al. (2019). Extracting tidal creek features in a heterogeneous background using Sentinel-2 imagery: a case study in the Yellow River Delta, China. International Journal of Remote Sensing.DOI:10.1080/01431161.2019.1707898

Zheng Y, Wu B F and Zhang M. (2017). Estimating the above ground biomass of winter wheat using the Sentinel-2 data. Journal of Remote Sensing, 21(2): 318–328. doi:10.11834/jrs.20176269

Zhou Z, Yang Y, Chen B. (2018). Estimating Spartina alterniflora fractional vegetation cover and aboveground biomass in a coastal wetland using SPOT6 satellite and UAV data. Aquatic Botany, 144:38-45.

**Table 1.** The number of sample data and verification data

| **Class** | **Sample Data** | **Sample Data** | **Sample Data** | **Verification Data** | **Verification Da** |
|---|---|---|---|---|---|
| | from on-site field | from high-resolution images | totally | from on-site field | from high-resoluti |
| P. australis | 105 | 145 | 250 | 270 | 230 |
| S. salsa | 120 | 130 | 250 | 390 | 110 |
| S. alterniflora | 150 | 100 | 250 | 200 | 300 |

**Table 2.** The statistics of classification accuracy

| **Species** | **Landsat-8** | **Landsat-8** | **Sentinel-2** | **Sentinel-2** |
|---|---|---|---|---|
| | PA/% | UA/% | PA/% | UA/% |
| *P. australis* | 73.80 | 70.83 | 81.60 | 76.55 |
| *S. salsa* | 72.80 | 70.82 | 79.20 | 79.04 |
| *S. alterniflora* | 76.60 | 79.79 | 82.20 | 83.37 |
| OA/% | 78.77 | 78.77 | 82.86 | 82.86 |
| Kappa | 0.74 | 0.74 | 0.79 | 0.79 |

**Table 3.** Landscape index of different vegetation communities during different years

| Species | CA | CA | CA | CA | PD | PD | PD | PD | LPI | LPI | LPI | LPI |
|---|---|---|---|---|---|---|---|---|---|---|---|---|
| | 2010 | 2013 | 2016 | 2018 | 2010 | 2013 | 2016 | 2018 | 2010 | 2013 | 2016 | 2018 |
| *S. salsa* | 47.60 | 27.48 | 39.61 | 35.04 | 23.21 | 27.07 | 13.13 | 11.81 | 2.85 | 1.70 | 3.70 | 2.11 |
| *P. australis* | 66.96 | 63.84 | 76.26 | 72.73 | 5.84 | 4.64 | 3.93 | 5.24 | 21.47 | 32.68 | 38.84 | 28.58 |
| *S. alterniflora* | 1.14 | 15.15 | 30.77 | 40.53 | 0.22 | 5.60 | 2.37 | 4.17 | 0.72 | 8.15 | 8.10 | 9.87 |

| Species | SPLIT | SPLIT | SPLIT | SPLIT | AI | AI | AI | AI |
|---|---|---|---|---|---|---|---|---|
| | 2010 | 2013 | 2016 | 2018 | 2010 | 2013 | 2016 | 2018 |
| *S. salsa* | 264.00 | 942.74 | 271.18 | 538.26 | 73.35 | 63.71 | 75.62 | 74.25 |
| *P. australis* | 12.34 | 8.60 | 6.38 | 11.26 | 91.96 | 90.23 | 92.55 | 88.53 |
| *S. alterniflora* | 181.80 | 139.83 | 87.79 | 56.55 | 88.52 | 87.95 | 92.73 | 92.14 |

**Table 4.** Standard deviation of elliptical parameters of spatial expansion of the S. alterniflora community in 2010-2018

| | North Bank of the Yellow River Delta | North Bank of the Yellow River Delta | North Bank of the Y |
|---|---|---|---|
| | Long semi-axis length (km) | Short semi-axis length (km) | Deflection angle (°) |
| 2010 | 0.52 | 0.12 | 100.41 |
| 2013 | 55.41 | 0.90 | 108.81 |
| 2016 | 63.30 | 22.40 | 89.35 |
| 2018 | 83.86 | 19.17 | 97.11 |

**Table 5.** Quantitative analysis of the spatial expansion pattern of S. alterniflora

| Expansion Mode | LEI range | Number of patches | Number of patches | Number of patches | Area ($km^2$) |
|---|---|---|---|---|---|
| | | **2010-2013** | **2013-2016** | **2016-2018** | **2010-2013** |
| Edge expansion | -1<LEI<0 | 0 | 20 | 25 | 0 |
| | 0[?]LEI<1 | 2 | 13 | 13 | 10.14 |
| External expansion | LEI=1 | 124 | 119 | 96 | 3.87 |

# Supporting Information

## 1.Characteristics of invasive species

The spatial and temporal distribution of wetland vegetation communities are affected by various factors, such as climate, hydrology, soil, topography, and the biological characteristics of vegetation itself. The distribution and growth situation of typical dominant communities in the Yellow River Delta wetland are as follows:

*S. salsa* (Fig. 1d) is a poly-salt and annual herbaceous plant with a flowering and fruiting period from July to October, and the entire plant turns red in summer and autumn. Because of its bubbles used for storing salt, it has strong salt tolerance and is the main coastal halophyte that is distributed in beach areas, without associated species. The height of the plant is in the range of 15–80 cm. Due to the influence of soil salinity

and groundwater depth, the vegetation coverage of the community is significantly different.

*P. australis* (Fig. 1e) is a perennial herbaceous plant that is mainly propagated by rhizomes. In early and mid-April, *P. australis* sprouts from underground rhizomes, with intense growth from April–July. The flowering and fruiting period is from August to September, and then the plant becomes dry and withered in October. The ecological range of *P. australis* is extremely wide, being distributed in the inland fresh water, coastal salt water, and brackish water interaction areas of the Yellow River Delta. With more than 50% coverage, the height of *P. australis* ranges from 0.5 to 3.0 m, with some plants exceeding 4 m.

*S. alterniflora* (Fig. 1f) is a perennial herbaceous plant that is salt-tolerant and resistant to wind and waves, is mainly distributed in the intertidal zone. The seeds can spread with the wind and waves. The roots are developed and often densely distributed in the soil layer to a depth of 30 cm. One plant can reproduce and yield dozens or even hundreds of plants within one year. The growth period of *S. alterniflora* is related to its geographical distribution. The jointing period of *S. alterniflora* in the study area is in early May, and the flowering period is from mid-August to early September. The seeds mature in mid- to late October, with the plant then entering the late growth stage and finally dying in November. With the height generally between 0.6–2.0 m and more than 90% coverage, the community composition of S. *alterniflora* is extremely simple, and it is an important invasive species in the Yellow River Delta Nature Reserve (Shi et al. 2009).

## 2.Data introduction

The Landsat-8 data and Sentinel-2 data used in this study were downloaded from the US Geological Survey official website (https://glovis.usgs.gov/) and the European Space Agency data sharing website (https://scihub.copernicus.eu/), respectively. The Landsat-8 image consisted of 8 bands at 30 m spatial resolution (Fig.S1). The area under study was covered by a single Landsat-8 image with path and row of 121/34. Atmospheric correction was performed for the Landsat-8 OLI image using the Fast Line-of-sight Atmospheric Analysis of Spectral Hypercube (FLAASH) model and Environment for Visualizing Images (ENVI) software (Shoko et al. 2017). The Sentinel-2 mission carries a multispectral instrument (MSI) with 13 spectral bands spanning from the visible spectrum (VIS) and near-infrared (NIR) to shortwave infrared (SWIR) at spatial resolutions of 10, 20, and 60 m (Yang et al. 2017; Yang et al. 2018) (Fig. 2). The Sentinel-2 dataset we downloaded was the standard product of the top of atmosphere (TOA) reflectance. Therefore, the atmospheric correction was preprocessed by the Sen2Cor model, which was utilized to transfer the TOA reflectance values to the bottom of atmosphere (BOA) reflectance values in the official software Sentinel Application Platform (SNAP) (Erinjery et al. 2018). After atmospheric correction, 20-m resolution bands, including bands 2-7, 8A, 11, and 12, were adopted for later extraction of native and invasive species.

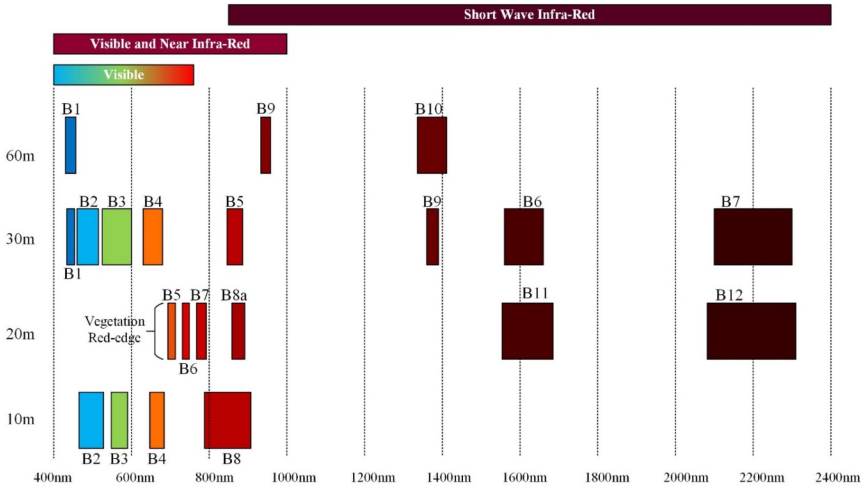

**Figure S1.** Spectral and spatial information for Sentinel-2 MSI and Landsat-8 OLI (Changed from Sentinel-2 MSI Level 2A Products Algorithm Theoretical Basis Document)

## 3.Method

### 3.1Random Forest

As a relatively new machine learning model, random forest can predict the role of up to several thousand variables and is regarded as one of the best machine learning algorithms. The random forest classification algorithm is an algorithm based on the classification and regression tree (CART) invented by Breiman et al., which integrates multiple decision trees through the idea of integrated learning. Its basic unit is the decision tree. If the CART decision tree is seen as an expert in the classification task, random forests are the experts that classify a task together (Iverson et al. 2008; Breiman 2001).

The steps for establishing a random forest are as follows:

(1) In the original sample, N training samples are randomly and regressively extracted, which is called the bootstrap method. This method is used to form a training sample set, and the data for each training sample set are approximately two-thirds of the original sample data set.

(2) Based on the extracted training sample set, N CART decision trees are constructed to form a random forest. During the decision tree growth process, m features are randomly selected at each node of each tree (the total number of features is M, m[?]M). According to the principle of minimum Gini coefficient, a feature with the most classification ability was selected to perform node splitting within the decision tree.

(3) Multiple decision trees are generated to form a random forest classifier, which is used to classify remote sensing images and determine the category by voting.

The random forest algorithm not only enables the classification of remote sensing images, but it also plays an important role in feature selection and dimensionality reduction. Since approximately one-third of the original sample data is not extracted during the sampling process, this part of the data is called the Out-Of-Bag data (OOB data). Out-Of-Bag-Error (OOB Error) generated by OOB data evaluates classification accuracy and also calculates the importance of different feature variables (Variable Important, VI) for feature selection (Genuer et al. 2010; Sandri et al. 2012). The characteristic variable importance assessment model is as follows:

$$\mathrm{VI}\,(M_A) = \frac{1}{N}\sum_{t=1}^{N}\,(B_{n_t}^{M_A} - B_{O_t}^{M_A}),$$

where $VI$ indicates the importance of the characteristic variable,$M$ is the total number of features of the sample, $N$ is the number of trees in the generated decision tree, $B_{O_t}^{M_A}$ is the OOB error of the t-th decision tree when any eigenvalue $M_A$ is not added with noise interference, and $B_{n_t}^{M_A}$ is the OOB error of the t-th decision tree when any eigenvalue $M_A$ is added with noise interference. If a certain feature $M_A$ is randomly added with noise, and the accuracy of the OOB data is greatly reduced, this indicates that the feature $M_A$ has a great influence on the classification result, and it also indicates that its importance is relatively high.

In the current study, the EnMAP-BOX tool developed by the German environment mapping and analysis program project team was used for band optimization and native and invasive species extraction. There are two important parameters in the process of constructing the random forest algorithm, namely, the number N of decision trees in the random forest and the number m of features extracted during the node-splitting process. When extracting feature variables, we selected the arithmetic square root of the total number of features in the EnMAP-BOX tool as the number of features. In theory, the greater the number of decision trees N, the higher the classification accuracy, but the higher the time cost. Based on the determination of the extracted feature m, we found that when the number of decision trees is N[?]20, the OOB error gradually converges and tends to be stable. Therefore, we chose N=20 as the number of generated decision trees.

### 3.2Accuracy assessment of species classification

The confusion matrix is also called the error matrix. It is mainly used to compare the degree of confusion between the classification result and the actual measured value for accuracy evaluation. In the current study, the overall accuracy (OA), Kappa coefficient, producer accuracy (PA), and user accuracy (UA), which are commonly used at present, were selected as evaluation indicators to evaluate the classification results of different remote sensing images.

### 3.3Landscape index

The landscape index refers to the highly concentrated landscape pattern information, which reflects the simple quantitative indicators of its structural composition and spatial configuration, and is suitable for quantitative spatial analysis of the relationship between landscape pattern and ecological process. Due to the large number of landscape indices, previous research was consulted, and the class area (CA), patch density (PD), largest patch index (LPI), splitting index (SPLIT), and aggregation index (AI) were selected for obtaining the spatial and temporal changes in the habitat pattern of native and invasive species (Zhen et al. 2012; Liu et al. 2017).

**Table S1.** Description of landscape index

| Landscape Index | Mathematical Model | Explanation | Explanation |
|---|---|---|---|
| Class Area | $N = \sum_{i=1}^{n} a_i$ | $N = \sum_{i=1}^{n} a_i$ | Total area of a certain type of |
| Patch Density | $PD = N/A$ | $PD = N/A$ | Indicates the number of patch |
| Largest Patch Index | $LPI = Max\ (a_1 \dots a_n)\ /A * 100$ | $LPI = Max\ (a_1 \dots a_n)\ /A * 100$ | Quantifies the percentage of to |
| Splitting Index | $SPLIT = A^2 / \sum_1^m a_i^2$ | $SPLIT = A^2 / \sum_1^m a_i^2$ | Indicates the degree of dispers |
| Aggregation Index | $AI = [\sum_{i=1}^{m} (g_{\mathrm{ii}}/maxg_{\mathrm{ii}})p_i] * 100$ | $AI = [\sum_{i=1}^{m} (g_{\mathrm{ii}}/maxg_{\mathrm{ii}})p_i] * 100$ | Reflects the proximity of the s |

$N$ is the total number of patches of the landscape type; $A$is the total area of the landscape type;$Max\ (a_1 \dots a_n)$ represents the area of the largest plaque;$E$ represents the total length of the landscape edge;$a_i$ represents the area of the $i$-$th$ plaque.$g_{\mathrm{ii}}$: Number of like adjacencies (joins) between pixels of patch type (class) $i$ based on the single-count method.max $g_{\mathrm{ii}}$: Maximum number of like adjacencies (joins) between pixels of patch type (class) $i$ based on the single-count method. $p_i$: Proportion of the landscape comprised of patch type (class) $i$ .

### 3.4Metrics for analysis of S.alterniflora expansion

#### 3.4.1 Standard deviational ellipse

The current study used the standard deviation ellipse to analyze the spatial variation characteristics of invasive species. This is a spatial statistical method that is used to quantitatively describe the spatial distribution characteristics of geographic elements, and is widely used in the fields of disease transmission, urban expansion, and pollution diffusion. The standard deviation ellipse parameters include the center of gravity coordinates, the deflection angle, and the length of the long and short half axes, which indicate the relative position of the spatial distribution pattern of geographic elements, the dominant trend direction of geographic element development, and the degree of dispersion in the primary and secondary directions, respectively. The calculation of key parameters can be found in previous studies (Wong 1999; Scott et al. 2010; Qiao et al. 2017).

#### 3.4.2 Metric for analysis of the spatial expansion of *S. alterniflora*

The pattern of landscape expansion determines the spatial combination of landscape elements, and the spatial combination of landscape elements has an important impact on various ecological processes. Therefore, the landscape expansion mode is of great significance for understanding the process of landscape expansion.

The landscape expansion index (LEI) was adopted to quantitatively realize the identification and analysis of landscape spatial expansion patterns (Liu et al. 2010; Wu et al. 2012). Its expression is as follows:

$LEI = \frac{A_p - A_0}{A_p + A_0}$,

where $A_p$ is the area of the expanded plaque, and $A_0$ is the area of the plaque adjacent to the expanded plaque, which can be understood as the original plaque. The range of the LEI is from -1 to 1 (including 1). When the LEI value is in the interval (-1, 1), we can call it edge expansion. When LEI<0, it indicates that the expansion area is smaller than the original plaque area. When LEI[?]0, it indicates that the expansion area is greater than or equal to the original plaque area. When LEI=1 ($A_0$=0), the original plaque does not exist, and the spatial expansion pattern of the*S. alterniflora* community is that of external expansion.

# References


Breiman L. (2001). Random Forests. Machine Learning, 45(1):5-32.

Erinjery J J , Mewa S , Rafi K. (2018). Mapping and assessment of vegetation types in the tropical rainforests of the Western Ghats using multispectral Sentinel-2 and SAR Sentinel-1 satellite imagery. Remote Sensing of Environment, 216:345-354.

Genuer, R, Poggi, J M and Tuleau-Malot C. (2010). Variable selection using random forests.Elsevier Science Inc.

Iverson L R , Prasad A M , Matthews S N , et al.(2008) Estimating potential habitat for 134 eastern US tree species under six climate scenarios. Forest Ecology and Management, 254(3):0-406.

Liu H Y, Lin Z S, Qi X Z, Liu J X, Xu X J. (2015) The dispersal mechanism of invasive plants based on a spatially explicit individual-based model and Remote sensing technology: a case study of Spartina alterniflora.Acta Ecologica Sinica, 35(23): 7794-7802. (in Chinese)

Liu S L, An N N, Yin Y J, Cheng F Y, Dong S K. (2017). Landscape pattern analysis and prediction of land-use change in the Guangxi coastal area. Acta Ecologica Sinica, 37(18): 5915-5923. (in Chinese)

Liu X, Li X, Chen Y , et al. (2010). A new landscape index for quantifying urban expansion using multi-temporal remotely sensed data. Landscape Ecology, 25(5):671-682.

Qiao K, Zhu W Q, Hu D Y, Hao M, Chen S S, Cao S S. (2017). Examining the distribution and dynamics of impervious surface in different functional zones of Beijing. ACTA GEOGRAPHICA SINICA, 72(11):2018-2031. (in Chinese)

Sandri M, Zuccolotto P. (2006). Variable Selection Using Random Forests. Data Analysis, Classification and the Forward Search.

Scott L M, Janikas M V. (2010). Spatial Statistics in ArcGIS. Handbook of Applied Spatial Analysis.

Shi D L, Tian J Y, Chen Y P. (2009). Biological and Ecological Characteristics of an Invasive Alien Species Spartina in Yellow River Delta. Journal of Binzho University, 25(03):27-32. (in Chinese)

Shoko, C., and Mutanga, O. (2017). Examining the strength of the newly-launched sentinel 2 msi sensor in detecting and discriminating subtle differences between c3 and c4 grass species. Isprs Journal of Photogrammetry & Remote Sensing, 129, 32-40.

Wong D W S. (1999). Several Fundamentals in Implementing Spatial Statistics in GIS: Using Centrographic Measures as Examples. Geographic Information Sciences, 5(2):163-174.

Wu P F, Zhou D M, Gong H L.(2012). A new landscape expansion index: definition and quantification. Acta Ecologica Sinica, 32(13): 4270-4277. (in Chinese)

Yang X., Zhao S., Qin X., Zhao N., Liang L. (2017). Mapping of Urban Surface Water Bodies from Sentinel-2 MSI Imagery at 10 m Resolution via NDWI-Based Image Sharpening. Remote Sensing. doi: 10.3390/rs9060596

Zhen Z, Gong Z N, Zhao W J. (2012). Analysis of Hydrophytes for Spatial Evolution Pattern in Guanting Reservoir, China. Journal of Agro-Environment Science. 31 (08):1586-1595. (in Chinese)

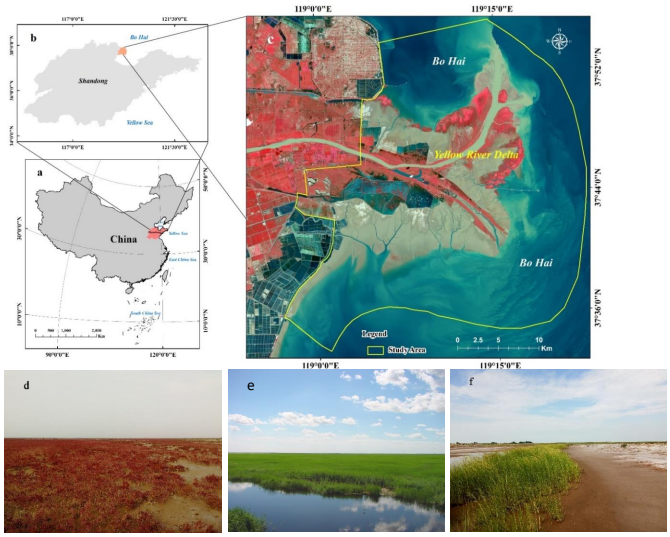


**Figure 1.** Location of the study area and field photos for (d) *S. salsa*, (e) *P. australis*, and (f) *S. alterniflora*

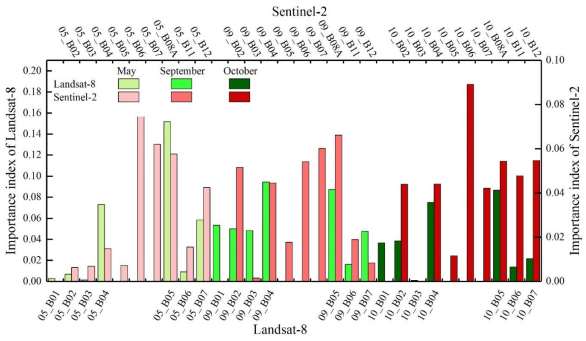


**Figure 2.** Importance of bands during different months from Sentinel-2 and Landsat-8 data.

Note: 05_B02 indicates the blue band of the image in May; 05_B03 indicates the green band of the image in May... and so on, as shown in the figure.



## Hosted file

`Figures.pdf` available at https://authorea.com/users/312565/articles/443137-extracting-spatiotemporal-characteristics-and-succession-pattern-of-native-and-invasive-plant-species-using-plant-phenophase-and-multi-source-remote-sensing-images-in-the-yellow-river-delta-china